

Superconductivity and magnetism/Supraconductivité et magnétisme

# Spin-polarized proximity effect in superconducting junctions

Takehito Yokoyama<sup>a,b</sup>, Yukio Tanaka<sup>a,b,\*</sup>

<sup>a</sup> Department of Applied Physics, Nagoya University, Nagoya 464-8603, Japan

<sup>b</sup> CREST, Japan Science and Technology Corporation (JST), Nagoya 464-8603, Japan

Available online 30 January 2006

## Abstract

We study spin dependent phenomena in superconducting junctions in both ballistic and diffusive regimes. For ballistic junctions we study both ferromagnet/*s*- and *d*-wave superconductor junctions and two-dimensional electron gas/*s*-wave superconductor junctions with Rashba spin-orbit coupling. It is shown that the exchange field always suppresses the conductance while the Rashba spin-orbit coupling can enhance it. In the latter part of the article we study the diffusive ferromagnet/insulator/*s*- and *d*-wave superconductor (DF/I/S) junctions, where the proximity effect can be enhanced by the exchange field in contrast to common belief. This resonant proximity effect in these junctions is studied for various situations: conductance of the junction and density of states of the DF are calculated by changing the heights of the insulating barriers at the interfaces, the magnitudes of the resistance in DF, the exchange field in DF, the transparencies of the insulating barriers and the angle between the normal to the interface and the crystal axis of *d*-wave superconductors  $\alpha$ . It is shown that the resonant proximity effect originating from the exchange field in DF strongly influences the tunneling conductance and density of states. We clarify the followings: for *s*-wave junctions, a sharp zero bias conductance peak (ZBCP) appears due to the resonant proximity effect. The magnitude of this ZBCP can exceed its value in normal states in contrast to that observed in diffusive normal metal/superconductor junctions. We find similar structures to the conductance in the density of states. For *d*-wave junctions at  $\alpha = 0$ , we also find a result similar to that in *s*-wave junctions. The magnitude of the resonant ZBCP at  $\alpha = 0$  can exceed that at  $\alpha/\pi = 0.25$  due to the formation of the mid gap Andreev resonant states. **To cite this article:** T. Yokoyama, Y. Tanaka, C. R. Physique 7 (2006).

© 2005 Académie des sciences. Published by Elsevier SAS. All rights reserved.

## Résumé

**Effets de proximité polarisés en spin dans les jonctions supraconductrices.** Nous étudions des phénomènes dépendant du spin dans des jonctions supraconductrices en régimes balistique et diffusif. Pour les jonctions balistiques, nous étudions à la fois les jonctions entre ferromagnétique et supraconducteurs à ondes *s* et *d* et entre gaz d'électrons bidimensionnel et supraconducteurs à ondes *s*, avec couplage spin-orbite de Rashba. Nous montrons que le champ d'échange diminue toujours la conductance alors que le couplage spin-orbite de Rashba peut l'augmenter. Dans le reste de l'article, nous étudions les jonctions diffusives ferromagnétique/isolant/supraconducteurs à ondes *s* et *d* (DF/I/S), où, contrairement à l'opinion commune, l'effet de proximité peut être accru par le champ d'échange. Cet effet de proximité résonnant dans ces jonctions est étudié dans diverses situations : la conductance de la jonction et la densité d'états du DF sont calculées en changeant les hauteurs des barrières isolantes aux interfaces, les amplitudes de la résistance dans DF, le champ d'échange dans DF, les transparences des barrières isolantes et l'angle  $\alpha$  entre la normale à l'interface et l'axe cristallographique des supraconducteurs à onde *d*. Nous montrons que l'effet de proximité résonnant dû au champ d'échange dans DF influence fortement la conductance tunnel et la densité d'états. Nous clarifions les points suivants : pour les jonctions à onde *s*, un pic marqué de conductance sous polarisation nulle (ZBCP) apparaît, à cause de l'effet

\* Corresponding author.

E-mail addresses: [h042224m@mbox.nagoya-u.ac.jp](mailto:h042224m@mbox.nagoya-u.ac.jp) (T. Yokoyama), [ytanaka@nuap.nagoya-u.ac.jp](mailto:ytanaka@nuap.nagoya-u.ac.jp) (Y. Tanaka).

de proximité résonnant. L'amplitude du ZBCP peut dépasser sa valeur dans les états normaux, à la différence de ce qui se produit dans les jonctions diffusives entre métal normal et supraconducteur. Nous trouvons des structures similaires à la conductance dans la densité d'états. Pour les jonctions à onde  $d$  à  $\alpha = 0$ , nous trouvons aussi un résultat similaire à celui obtenu pour les jonction à onde  $s$ . L'amplitude du ZBCP résonnant à  $\alpha = 0$  peut être supérieure à celle obtenue à  $\alpha/\pi = 0,25$ , à cause de l'apparition d'états d'Andreev résonnants en milieu de bande interdite. *Pour citer cet article : T. Yokoyama, Y. Tanaka, C. R. Physique 7 (2006).*  
 © 2005 Académie des sciences. Published by Elsevier SAS. All rights reserved.

*Keywords:* Andreev reflection; Proximity effect; Mid gap Andreev resonant states; Exchange field; Rashba spin-orbit coupling

*Mots-clés :* Réflexion d'Andreev ; États d'Andreev résonnants en milieu de bande interdite ; Champ d'échange ; Couplage spin-orbite de Rashba

## 1. Introduction

In normal metal/superconductor (N/S) junctions, a unique scattering process occurs in low energy transport: Andreev reflection (AR) [1]. The AR is a process where an electron injected from N with energy below the energy gap  $\Delta$  is converted into a reflected hole. Taking the AR into account, Blonder, Tinkham and Klapwijk (BTK) proposed the formula for the calculation of the tunneling conductance [2]. It revealed the gap-like structure or the doubling of tunneling conductance due to the AR. This method was extended to normal metal/unconventional superconductor (N/US) junctions [3]. It is shown that a zero bias conductance peak (ZBCP) appears when the mid gap Andreev resonant state (MARS) is formed due to the anisotropy of US.

The BTK theory was also extended to ferromagnet/superconductor (F/S) or ferromagnet/unconventional superconductor (F/US) junctions [4] and used to estimate the spin polarization of the F layer experimentally [5–7]. In F/S junctions, AR is suppressed because the retro-reflectivity is broken by the spin-polarization in the F layer [8]. To clarify spin dependent transport phenomena is important for the fabrication of a new device manipulating an electron's spin. Nowadays, there are many works about charge transport of electrons relevant to electron spin.

Among recent works, many efforts have been devoted to study the effect of spin-orbit coupling on transport properties of two-dimensional electron gas (2DEG) [9–12]. The pioneering work by Datta and Das suggested the way to control the precession of the spins of electrons by the Rashba spin-orbit coupling (RSOC) [13] in F/2DEG/F junctions [14]. This spin-orbit coupling depends on the applied field and can be tuned by a gate voltage. It also gives the off-diagonal elements of the velocity operator [15]. There are several works about spin dependent transport in the presence of RSOC [16,17].

The RSOC induces an energy splitting, but the energy splitting does not break the time reversal symmetry unlike an exchange splitting in ferromagnet. Therefore transport properties in 2DEG/S junctions may be qualitatively different from those in F/S junctions. As far as we know, in 2DEG/S junctions the effect of RSOC on transport phenomena is not studied well. Recent experimental and theoretical advances in spintronics stimulate us to challenge this problem. We illustrate the two kinds of splittings in Fig. 1.

The first purpose of this article is to calculate the tunneling conductance in F/S and 2DEG/S junctions and clarify how the exchange field and the RSOC affect it. We think the obtained results are useful for a better understanding of related experiments in mesoscopic F/S and 2DEG/S junctions.

On the other hand, in diffusive junctions, the physics is clearly different from that in ballistic junctions. In diffusive normal metal/superconductor (DN/S) junctions, proximity effects play an important role in the low energy transport.

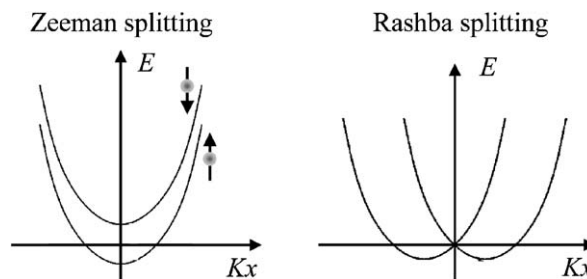


Fig. 1. Zeeman versus Rashba splitting.

The phase coherence between incoming electrons and Andreev reflected holes persists in DN at a mesoscopic length scale and results in strong interference effects on the probability of AR [18]. One of the striking experimental manifestations is the zero bias conductance peak (ZBCP) [19–29].

A quasiclassical Green's function theory [30–32] is often applied to the charge transport in DN/S junctions. Volkov, Zaitsev and Klapwijk (VZK) solved the Usadel equations [33], and showed that this ZBCP is due to the enhancement of the pair amplitude in DN by the proximity effect [34]. VZK applied the Kupriyanov and Lukichev (KL) boundary condition for the Keldysh–Nambu Green's function [35]. Stimulated by the VZK theory, several authors studied the charge transport in various junctions [36–44].

Recently one of the authors [45] developed the VZK theory for  $s$ -wave superconductors using more general boundary conditions provided by the circuit theory of Nazarov [46]. The boundary conditions coincide with the KL conditions when a connector is diffusive with low transparent coefficients, while the BTK theory [2] is reproduced in the ballistic regime. The extended VZK theory [45] produced a crossover from a ZBCP to a zero bias conductance dip (ZBCD). These phenomena are relevant for the actual junctions in which the barrier transparency is not necessarily small.

The formation of the MARS at the interface of unconventional superconductors [47,3,48,49] also generates the ZBCP as mentioned above. The generalized VZK theory was recently applied to unconventional superconducting junctions [50–52]. The formation of the MARS is naturally taken into account in this approach. It was demonstrated that the formation of MARS in DN/ $d$ -wave superconductor (DN/D) junctions strongly competes with the proximity effect.

The above theories treat spin independent phenomena in diffusive junctions. Calculations of tunneling conductance in the presence of the magnetic impurities in DN/S junctions were performed in [53,54,34]. Spin dependent transport is also realized in ferromagnet/superconductor junctions.

In diffusive ferromagnet/superconductor (DF/S) junctions Cooper pairs penetrate into the DF layer from the S layer and have a nonzero momentum by the exchange field [55–57]. This property produces many interesting phenomena [58–72]. One interesting consequence of the oscillations of the pair amplitude is the spatially damped oscillating behavior of the density of states (DOS) in a ferromagnet predicted theoretically [73–76]. In the ferromagnet the exchange field usually breaks the induced Cooper pairs. However, for a weak exchange field, the pair amplitude can be *enhanced* and the energy dependent DOS can have a zero-energy peak [77]. The DOS has been studied extensively [74,77–79] but the condition for the appearance of the DOS peak was not studied systematically. We studied the conditions for the appearance of such anomaly, i.e., strong enhancement of the proximity effect and found two conditions corresponding to weak proximity effect and strong one [80]. Since DOS is a fundamental quantity, this *resonant proximity effect* can influence various transport phenomena.

Another purpose of the present article is to study the influence of the resonant proximity effect by the exchange field on the tunneling conductance and the DOS in DF/ $s$ - and  $d$ -wave superconductor junctions with Nazarov's boundary conditions. A weak exchange field is realized in recent experiments with, e.g., Ni doped Pd [79] or magnetic semiconductor. Thus our results may be observed in experiments. In the latter part of this article we calculate the tunneling conductance and the density of states in normal metal/insulator/diffusive ferromagnet/insulator/ $s$ - and  $d$ -wave superconductor (N/I/DF/I/S) junctions for various parameters such as the heights of the insulating barriers at the interfaces, resistance  $R_d$  in DF, the exchange field  $h$  in DF, the Thouless energy  $E_{Th}$  in DF, the transparencies of the insulating barriers and the angle between the normal to the interface and the crystal axis of  $d$ -wave superconductors  $\alpha$ . Throughout the article we confine ourselves to zero temperature.

The organization of this article is as follows. In Sections 2 and 3, we will provide the detailed derivation of the expression for the normalized tunneling conductance and the results of calculations are presented for various types of junctions, in ballistic and diffusive junctions respectively. In Section 4, the summary of the obtained results is given.

## 2. Ballistic junctions

We consider F/S and F/ $d$ -wave superconductor (F/D) junctions. We use the same method as in [4] and the same notations. In the following  $\uparrow$  ( $\downarrow$ ) denotes majority (minority) spin. The F/US interface located at  $x = 0$  (the  $y$ -axis) has

an infinitely narrow insulating barrier described by the delta function  $U(x) = H\delta(x)$ . As a model of the ferromagnet we apply the Stoner model with the exchange potential  $U$ . The pair potential matrix we consider is given by

$$\widehat{\Delta}(\theta) = \begin{pmatrix} 0 & \Delta_{\uparrow\downarrow}(\theta) \\ \Delta_{\uparrow\downarrow}(\theta) & 0 \end{pmatrix} \quad (1)$$

where  $\theta$  denotes the direction of motions of quasiparticles measured from the normal to the interface. Below we consider  $s$ - and  $d$ -wave superconductors. The pair potentials are given by  $\Delta_{\downarrow\uparrow} = -\Delta_{\uparrow\downarrow} = \Delta$  for  $s$ -wave superconductors and  $\Delta_{\downarrow\uparrow} = -\Delta_{\uparrow\downarrow} = \Delta \cos[2(\theta - \alpha)]$  for  $d$ -wave superconductors where  $\alpha$  denotes the angle between the normal to the interface and the crystal axis of  $d$ -wave superconductors. Here  $\Delta$  denotes the energy gap.

Applying the BTK method [2,4], we obtain the conductance  $\sigma_{S\uparrow(\downarrow)}$  for up (down) spin quasiparticle represented in the form:

$$\begin{aligned} \sigma_{S\uparrow} = & \sigma_{N\uparrow} \frac{1 - |\Gamma_+ \Gamma_-|^2 (1 - \sigma_{N\downarrow}) + \sigma_{N\downarrow} |\Gamma_+|^2}{|1 - \Gamma_+ \Gamma_- \sqrt{1 - \sigma_{N\uparrow}} \sqrt{1 - \sigma_{N\downarrow}} \exp[i(\varphi_{\downarrow} - \varphi_{\uparrow})]|^2} \Theta(\theta_C - |\theta|) \\ & + \sigma_{N\uparrow} \frac{1 - |\Gamma_+ \Gamma_-|^2}{|1 - \Gamma_+ \Gamma_- \sqrt{1 - \sigma_{N\uparrow}} \exp[i(\varphi_{\downarrow} - \varphi_{\uparrow})]|^2} \Theta(|\theta| - \theta_C) \end{aligned} \quad (2)$$

$$\sigma_{S\downarrow} = \sigma_{N\downarrow} \frac{1 - |\Gamma_+ \Gamma_-|^2 (1 - \sigma_{N\uparrow}) + \sigma_{N\uparrow} |\Gamma_+|^2}{|1 - \Gamma_+ \Gamma_- \sqrt{1 - \sigma_{N\uparrow}} \sqrt{1 - \sigma_{N\downarrow}} \exp[i(\varphi_{\uparrow} - \varphi_{\downarrow})]|^2} \Theta(\theta_C - |\theta|) \quad (3)$$

$$\exp(i\varphi_{\downarrow}) = \frac{1 - \lambda_- + iZ\theta}{\sqrt{1 - \sigma_{N\downarrow}}(1 + \lambda_- - iZ\theta)}, \quad \exp(-i\varphi_{\uparrow}) = \frac{1 - \lambda_+ - iZ\theta}{\sqrt{1 - \sigma_{N\uparrow}}(1 + \lambda_+ + iZ\theta)} \quad (4)$$

$$\Gamma_{\pm} = \frac{\Delta_{\pm}(\theta)}{E + \sqrt{E^2 - |\Delta_{\pm}(\theta)|^2}} \quad (5)$$

where  $Z\theta = \frac{Z}{\cos\theta}$ ,  $Z = \frac{2mH}{\hbar^2 k_F}$  and  $\theta_C = \cos^{-1} \sqrt{U/E_F}$  with quasiparticle energy  $E$ , effective mass  $m$ , Fermi wavenumber  $k_F$  and Fermi energy  $E_F$ . In the above,  $\Theta(x)$  is the Heaviside step function and  $\sigma_{N\uparrow(\downarrow)}$  denotes the conductance for up (down) spin quasiparticle in the normal state:

$$\sigma_{N\uparrow} = \frac{4\lambda_+}{(1 + \lambda_+)^2 + Z_{\theta}^2}, \quad \sigma_{N\downarrow} = \frac{4\lambda_-}{(1 + \lambda_-)^2 + Z_{\theta}^2} \Theta(\theta_C - |\theta|) \quad (6)$$

with  $\lambda_{\pm} = \sqrt{1 \pm \frac{U}{E_F \cos^2 \theta}}$ .

Normalized conductance is expressed as

$$\sigma_T = \frac{\int_{-\pi/2}^{\pi/2} d\theta \cos\theta (\sigma_{S\uparrow} + \sigma_{S\downarrow})}{\int_{-\pi/2}^{\pi/2} d\theta \cos\theta (\sigma_{N\uparrow} + \sigma_{N\downarrow})} \quad (7)$$

Next we consider a ballistic 2DEG/S junctions. The 2DEG/S interface located at  $x = 0$  (along the  $y$ -axis) has an infinitely narrow insulating barrier described by the delta function  $U(x) = H\delta(x)$ . The effective Hamiltonian with RSOC is given by

$$H = \begin{pmatrix} \xi_k & i\lambda k_- \Theta(-x) & 0 & \Delta \Theta(x) \\ -i\lambda k_+ \Theta(-x) & \xi_k & -\Delta \Theta(x) & 0 \\ 0 & -\Delta \Theta(x) & -\xi_k & -i\lambda k_+ \Theta(-x) \\ \Delta \Theta(x) & 0 & i\lambda k_- \Theta(-x) & -\xi_k \end{pmatrix} \quad (8)$$

with  $k_{\pm} = k_x \pm ik_y$ ,  $\xi_k = \frac{\hbar^2}{2m}(k^2 - k_F^2)$ , Fermi wave number  $k_F$ , Rashba coupling constant  $\lambda$ .

The velocity operator in the  $x$ -direction is given by [15]:

$$v_x = \frac{\partial H}{\hbar \partial k_x} = \begin{pmatrix} \frac{\hbar}{mi} \frac{\partial}{\partial x} & \frac{i\lambda}{\hbar} \Theta(-x) & 0 & 0 \\ -\frac{i\lambda}{\hbar} \Theta(-x) & \frac{\hbar}{mi} \frac{\partial}{\partial x} & 0 & 0 \\ 0 & 0 & -\frac{\hbar}{mi} \frac{\partial}{\partial x} & -\frac{i\lambda}{\hbar} \Theta(-x) \\ 0 & 0 & \frac{i\lambda}{\hbar} \Theta(-x) & -\frac{\hbar}{mi} \frac{\partial}{\partial x} \end{pmatrix} \quad (9)$$

The wave function  $\psi(x)$  for  $x \leq 0$  (2DEG region) is represented using eigenfunctions of the Hamiltonian:

$$e^{ik_y y} \left[ \frac{1}{\sqrt{2}} e^{ik_1(2) \cos \theta_1 x} \begin{pmatrix} (-i) \frac{k_1(2)-}{k_1(2)} \\ 1 \\ 0 \\ 0 \end{pmatrix} + \frac{a_1(2)}{\sqrt{2}} e^{ik_1 \cos \theta_1 x} \begin{pmatrix} 0 \\ 0 \\ i \frac{k_1+}{k_1} \\ 1 \end{pmatrix} + \frac{b_1(2)}{\sqrt{2}} e^{ik_2 \cos \theta_2 x} \begin{pmatrix} 0 \\ 0 \\ -i \frac{k_2+}{k_2} \\ 1 \end{pmatrix} \right. \\ \left. + \frac{c_1(2)}{\sqrt{2}} e^{-ik_1 \cos \theta_1 x} \begin{pmatrix} -i \frac{k_1+}{k_1} \\ 1 \\ 0 \\ 0 \end{pmatrix} + \frac{d_1(2)}{\sqrt{2}} e^{-ik_2 \cos \theta_2 x} \begin{pmatrix} i \frac{k_2+}{k_2} \\ 1 \\ 0 \\ 0 \end{pmatrix} \right] \quad (10)$$

for an injection wave with wave number  $k_1(2)$  where

$$k_1 = -m\lambda/\hbar^2 + \sqrt{(m\lambda/\hbar^2)^2 + k_F^2}, \quad k_2 = m\lambda/\hbar^2 + \sqrt{(m\lambda/\hbar^2)^2 + k_F^2}$$

and  $k_{1(2)\pm} = k_{1(2)} e^{\pm i\theta_{1(2)}}$ .  $a_1(2)$  and  $b_1(2)$  are AR coefficients.  $c_1(2)$  and  $d_1(2)$  are normal reflection coefficients.  $\theta_{1(2)}$  is an angle of the wave with wave number  $k_{1(2)}$  with respect to the interface normal.

Similarly for  $x \geq 0$ ,  $\psi(x)$  (S region) is given by the linear combination of the eigenfunctions. Note that since the translational symmetry holds for the  $y$ -direction, the momenta parallel to the interface are conserved:  $k_y = k_F \sin \theta = k_1 \sin \theta_1 = k_2 \sin \theta_2$ .

The wave function follows the boundary conditions [15]:

$$\psi(x)|_{x=+0} = \psi(x)|_{x=-0} \quad (11)$$

$$v_x \psi(x)|_{x=+0} - v_x \psi(x)|_{x=-0} = \frac{\hbar}{m i} \frac{2mU}{\hbar^2} \begin{pmatrix} 1 & 0 & 0 & 0 \\ 0 & 1 & 0 & 0 \\ 0 & 0 & -1 & 0 \\ 0 & 0 & 0 & -1 \end{pmatrix} \psi(0) \quad (12)$$

Applying BTK theory to our calculation, we obtain the dimensionless conductance represented in the form:

$$\sigma_s = N_1 \int_{-\theta_C}^{\theta_C} \frac{1}{2} [K_{21} + |a_1|^2 K_{21} + |b_1|^2 K_{12} \lambda_{21} - |c_1|^2 K_{21} - |d_1|^2 K_{12} \lambda_{21}] \cos \theta \, d\theta \\ + N_2 \int_{-\pi/2}^{\pi/2} \text{Re} \frac{1}{2} [K_{12} + |a_2|^2 K_{21} \lambda_{12} + |b_2|^2 K_{12} - |c_2|^2 K_{21} \lambda_{12} - |d_2|^2 K_{12}] \cos \theta \, d\theta \quad (13)$$

with  $K_{12} = 1 + k_1/k_2$ ,  $K_{21} = 1 + k_2/k_1$  and

$$\lambda_{12} = \frac{k_1 \cos \theta_1}{k_2 \cos \theta_2}; \quad \lambda_{21} = \frac{k_2 \cos \theta_2}{k_1 \cos \theta_1}; \quad N_1 = \frac{1}{1 + \frac{m\lambda}{\hbar^2 k_1}}; \quad N_2 = \frac{1}{1 - \frac{m\lambda}{\hbar^2 k_2}} \quad (14)$$

$N_1$  and  $N_2$  are normalized density of states for wave number  $k_1$  and  $k_2$  respectively. The critical angle  $\theta_C$  is defined as  $\cos \theta_C = \sqrt{\frac{2m\lambda}{\hbar^2 k_1}}$ .

$\sigma_N$  is given by the conductance for normal states, i.e.,  $\sigma_S$  for  $\Delta = 0$ . We define normalized conductance as  $\sigma_T = \sigma_S/\sigma_N$  and a parameter  $\beta$  as  $\beta = \frac{2m\lambda}{\hbar^2 k_F}$ .

First we study the difference between the effect of the Zeeman splitting and that of Rashba splitting. We plot the tunneling conductance for superconducting states,  $\sigma_S$  for F/S junctions in (a)–(c) and for 2DEG/S junctions in (d)–(f) of Fig. 2 with  $Z = 10$  in (a) and (d),  $Z = 1$  in (b) and (e), and  $Z = 0$  in (c) and (f). The exchange field suppresses  $\sigma_S$  independently of  $Z$  as shown in (a)–(c). This is because the AR probability is reduced by the exchange field. On the other hand the dependence of  $\sigma_S$  on  $\beta$  at zero voltage is qualitatively different. In (d)–(f) we show the dependence of  $\sigma_S$  on  $\beta$  at zero voltage for various  $Z$ . For  $Z = 10$  it has an exponential dependence on  $\beta$  but its magnitude is very

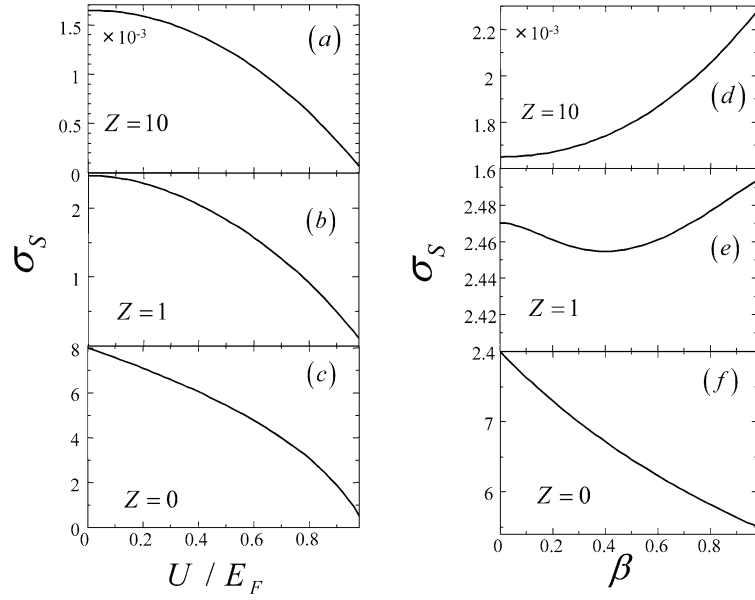


Fig. 2. Tunneling conductance for superconducting states at zero voltage as a function of the exchange field in F/S junctions (left panels) and RSOC in 2DEG/S junctions (right panels) with  $Z = 10$  in (a) and (d),  $Z = 1$  in (b) and (e), and  $Z = 0$  in (c) and (f).

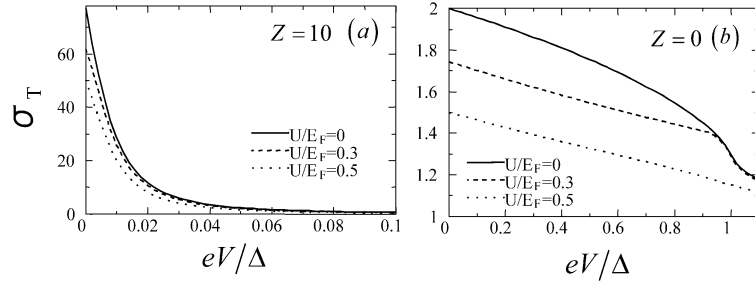


Fig. 3. Normalized tunneling conductance in F/D junctions at  $\alpha/\pi = 0.25$  with  $Z = 10$  in (a) and  $Z = 0$  in (b).

small. For  $Z = 1$  it has a re-entrant behavior as a function of  $\beta$ . For  $Z = 0$  it decreases linearly as a function of  $\beta$ . The AR probability is enhanced by the RSOC at  $Z = 10$ .

Next we will study the F/D junctions. The normalized tunneling conductance  $\sigma_T$  as a function of bias voltage  $V$  is plotted in Fig. 3 for  $\alpha/\pi = 0.25$  and various exchange field with  $Z = 10$  in (a) and  $Z = 0$  in (b). For  $Z = 10$  a ZBCP appears due to the formation of the MARS as shown in (a). As the exchange field increases,  $\sigma_T$  is suppressed. Similar plots at  $Z = 0$  are shown in (b). We can find that  $\sigma_T$  decreases with the increase of the exchange field.

### 3. Diffusive junctions

We consider a junction consisting of normal and superconducting reservoirs connected by a quasi-one-dimensional diffusive ferromagnet conductor (DF) with a length  $L$  much larger than the mean free path. The interface between the DF conductor and the S electrode has a resistance  $R_b$  while the DF/N interface has a resistance  $R'_b$ . The positions of the DF/N interface and the DF/S interface are denoted as  $x = 0$  and  $x = L$ , respectively. We model infinitely narrow insulating barriers by the delta function  $U(x) = H\delta(x - L) + H'\delta(x)$ . The resulting transparency of the junctions  $T_m$  and  $T'_m$  are given by  $T_m = 4 \cos^2 \phi / (4 \cos^2 \phi + Z^2)$  and  $T'_m = 4 \cos^2 \phi / (4 \cos^2 \phi + Z'^2)$ , where  $Z = 2H/v_F$  and  $Z' = 2H'/v_F$  are dimensionless constants and  $\phi$  is the injection angle measured from the interface normal to the junction and  $v_F$  is Fermi velocity.

We apply the quasiclassical Keldysh formalism in the following calculation of the tunneling conductance. The  $4 \times 4$  Green's functions in N, DF and S are denoted by  $\check{G}_0(x)$ ,  $\check{G}_1(x)$  and  $\check{G}_2(x)$  respectively where the Keldysh component  $\hat{K}_{0,1,2}(x)$  is given by  $\hat{K}_i(x) = \hat{R}_i(x)\hat{f}_i(x) - \hat{f}_i(x)\hat{A}_i(x)$  with retarded component  $\hat{R}_i(x)$ , advanced component  $\hat{A}_i(x) = -\hat{R}_i^*(x)$  using distribution function  $\hat{f}_i(x)$  ( $i = 0, 1, 2$ ). In the above,  $\hat{R}_0(x)$  is expressed by  $\hat{R}_0(x) = \hat{\tau}_3$  and  $\hat{f}_0(x) = f_0 + \hat{\tau}_3 f_{i0}$ .  $\hat{R}_2(x)$  is expressed by  $\hat{R}_2(x) = g\hat{\tau}_3 + f\hat{\tau}_2$  with  $g = \varepsilon/\sqrt{\varepsilon^2 - \Delta^2}$  and  $f = \Delta/\sqrt{\Delta^2 - \varepsilon^2}$ , where  $\hat{\tau}_2$  and  $\hat{\tau}_3$  are the Pauli matrices, and  $\varepsilon$  denotes the quasiparticle energy measured from the Fermi energy and  $\hat{f}_2(x) = \tanh[\varepsilon/(2T)]$  in thermal equilibrium with temperature  $T$ . We put the electrical potential zero in the S-electrode. In this case, the spatial dependence of  $\check{G}_1(x)$  in DF is determined by the static Usadel equation [33],

$$D \frac{\partial}{\partial x} \left[ \check{G}_1(x) \frac{\partial \check{G}_1(x)}{\partial x} \right] + i[\check{H}, \check{G}_1(x)] = 0 \quad (15)$$

with the diffusion constant  $D$  in DF. Here  $\check{H}$  is given by

$$\check{H} = \begin{pmatrix} \hat{H}_0 & 0 \\ 0 & \hat{H}_0 \end{pmatrix} \quad (16)$$

with  $\hat{H}_0 = (\varepsilon + (-)h)\hat{\tau}_3$  for majority (minority) spin where  $h$  denotes the exchange field. Note that we assume a weak ferromagnet and neglect the difference of Fermi velocity between majority spin and minority spin. The Nazarov's generalized boundary condition for  $\check{G}_1(x)$  at the DF/S interface is given by [45,51]. We also use Nazarov's generalized boundary condition for  $\check{G}_1(x)$  at the DF/N interface:

$$\frac{L}{R_d} \left( \check{G}_1 \frac{\partial \check{G}_1}{\partial x} \right) \Big|_{x=0_+} = -R_b'^{-1} \langle B \rangle', \quad B = \frac{2T_m' [\check{G}_0(0_-), \check{G}_1(0_+)]}{4 + T_m' ([\check{G}_0(0_-), \check{G}_1(0_+)]_+ - 2)} \quad (17)$$

The average over the various angles of injected particles at the interface is defined as

$$\langle B(\phi) \rangle^{(l)} = \frac{\int_{-\pi/2}^{\pi/2} d\phi \cos \phi B(\phi)}{\int_{-\pi/2}^{\pi/2} d\phi T^{(l)}(\phi) \cos \phi} \quad (18)$$

with  $B(\phi) = B$  and  $T^{(l)}(\phi) = T_m^{(l)}$ . The resistance of the interface  $R_b^{(l)}$  is given by

$$R_b^{(l)} = R_0^{(l)} \frac{2}{\int_{-\pi/2}^{\pi/2} d\phi T^{(l)}(\phi) \cos \phi} \quad (19)$$

Here  $R_0^{(l)}$  is Sharvin resistance, which in three-dimensional case is given by  $R_0^{(l)-1} = e^2 k_F^2 S_c^{(l)} / (4\pi^2)$ , where  $k_F$  is the Fermi wave-vector and  $S_c^{(l)}$  is the constriction area. Note that the area  $S_c^{(l)}$  is, in general, not equal to the cross-section area  $S_d$  of the normal conductor, therefore  $S_c^{(l)} / S_d$  is independent parameter of our theory. This allows us to vary  $R_d / R_b^{(l)}$  independently of  $T_m^{(l)}$ . In the real physical situation, the assumption  $S_c^{(l)} < S_d$  means that only a part of the actual flat DN/S interface (having area  $S_c^{(l)}$ ) is conducting whether it is a single conducting region or a series of such regions. These conducting regions are not constrictions in a standard sense—we do not assume the narrowing of the total cross-section, but rather that only the part of the cross-section is conducting.

The electric current per one spin is expressed using  $\check{G}_1(x)$  as

$$I_{el} = \frac{-L}{8eR_d} \int_0^\infty d\varepsilon \text{Tr} \left[ \hat{\tau}_3 \left( \check{G}_1(x) \frac{\partial \check{G}_1(x)}{\partial x} \right)^K \right] \quad (20)$$

where  $(\check{G}_1(x) \frac{\partial \check{G}_1(x)}{\partial x})^K$  denotes the Keldysh component of  $(\check{G}_1(x) \frac{\partial \check{G}_1(x)}{\partial x})$ . In the actual calculation it is convenient to use the standard  $\theta$ -parameterization where the retarded Green's function  $\hat{R}_1(x)$  is expressed as  $\hat{R}_1(x) = \hat{\tau}_3 \cos \theta(x) + \hat{\tau}_2 \sin \theta(x)$ . The parameter  $\theta(x)$  is a measure of the proximity effect in DF.

The distribution function  $\hat{f}_1(x)$  is given by  $\hat{f}_1(x) = f_1(x) + \hat{\tau}_3 f_i(x)$ . In the above,  $f_i(x)$  is the relevant distribution function which determines the conductance of the junction we are now concentrating on. From the retarded or advanced component of the Usadel equation, the spatial dependence of  $\theta(x)$  is determined by the following equation

$$D \frac{\partial^2}{\partial x^2} \theta(x) + 2i(\varepsilon + (-)h) \sin[\theta(x)] = 0 \quad (21)$$

for majority (minority) spin, while for the Keldysh component we obtain

$$D \frac{\partial}{\partial x} \left[ \frac{\partial f_i(x)}{\partial x} \cosh^2 \theta_{\text{im}}(x) \right] = 0 \quad (22)$$

At  $x = 0$ , since  $f_{i0}$  is the distribution function in the normal electrode, it is satisfied with

$$f_{i0} = \frac{1}{2} \left\{ \tanh[(\varepsilon + eV)/(2T)] - \tanh[(\varepsilon - eV)/(2T)] \right\} \quad (23)$$

Next we focus on the boundary condition at the DF/N interface. Taking the retarded part of Eq. (17), we obtain

$$\frac{L}{R_d} \frac{\partial \theta(x)}{\partial x} \Big|_{x=0_+} = \frac{\langle F \rangle'}{R_b'} F = \frac{2T_m' \sin \theta_0}{(2 - T_m') + T_m' \cos \theta_0} \quad (24)$$

with  $\theta_0 = \theta(0_+)$ .

On the other hand, from the Keldysh part of Eq. (17), we obtain

$$\frac{L}{R_d} \left( \frac{\partial f_i}{\partial x} \right) \cosh^2 \theta_{\text{im}}(x) \Big|_{x=0_+} = - \frac{\langle I_{b1} \rangle' (f_{i0} - f_i(0_+))}{R_b'}, \quad I_{b1} = \frac{T_m'^2 \Lambda_1' + 2T_m' (2 - T_m') \text{Real}\{\cos \theta_0\}}{|(2 - T_m') + T_m' \cos \theta_0|^2} \quad (25)$$

$$\Lambda_1' = (1 + |\cos \theta_0|^2 + |\sin \theta_0|^2) \quad (26)$$

After some calculations we obtain the following final result for the current:

$$I_{\text{el}} = \frac{1}{2e} \int_0^\infty d\varepsilon \frac{f_{i0}}{\frac{R_b}{\langle I_{b0} \rangle} + \frac{R_d}{L} \int_0^L \frac{dx}{\cosh^2 \theta_{\text{im}}(x)} + \frac{R_b'}{\langle I_{b1} \rangle'}} \quad (27)$$

Then the differential resistance  $R$  per one spin projection at zero temperature is given by

$$R = \frac{2R_b}{\langle I_{b0} \rangle} + \frac{2R_d}{L} \int_0^L \frac{dx}{\cosh^2 \theta_{\text{im}}(x)} + \frac{2R_b'}{\langle I_{b1} \rangle'} \quad (28)$$

with

$$I_{b0} = \frac{T_m'^2 \Lambda_1 + 2T_m (2 - T_m) \Lambda_2}{2|(2 - T_m) + T_m [g \cos \theta_L + f \sin \theta_L]|^2} \quad (29)$$

$$\Lambda_1 = (1 + |\cos \theta_L|^2 + |\sin \theta_L|^2) (|g|^2 + |f|^2 + 1) + 4 \text{Imag}[fg^*] \text{Imag}[\cos \theta_L \sin \theta_L^*] \quad (30)$$

$$\Lambda_2 = \text{Real}\{g(\cos \theta_L + \cos \theta_L^*) + f(\sin \theta_L + \sin \theta_L^*)\} \quad (31)$$

This is an extended version of the VZK formula [34]. In the above  $\theta_{\text{im}}(x)$  and  $\theta_L$  denote the imaginary part of  $\theta(x)$  and  $\theta(L_-)$ , respectively. Then the total tunneling conductance in the superconducting state  $\sigma_S(eV)$  is given by  $\sigma_S(eV) = \sum_{\uparrow, \downarrow} 1/R$ . The local normalized DOS  $N(\varepsilon)$  in the DF layer is given by

$$N(\varepsilon) = \frac{1}{2} \sum_{\uparrow, \downarrow} \text{Re} \cos \theta(x). \quad (32)$$

It is important to note that in the present approach, according to circuit theory,  $R_d/R_b^{(l)}$  can be varied independently of  $T_m^{(l)}$ , i.e., independently of  $Z^{(l)}$ , since one can change the magnitude of the constriction area  $S_c^{(l)}$  independently. In other words,  $R_d/R_b^{(l)}$  is no more proportional to  $T_{\text{av}}^{(l)}(L/l)$ , where  $T_{\text{av}}^{(l)}$  is the averaged transmissivity of the barrier and  $l$  is the mean free path in the diffusive region. Based on this fact, we can choose  $R_d/R_b^{(l)}$  and  $Z^{(l)}$  as independent parameters.

In the following, we will discuss the normalized tunneling conductance  $\sigma_T(eV) = \sigma_S(eV)/\sigma_N(eV)$  where  $\sigma_N(eV)$  is the tunneling conductance in the normal state given by  $\sigma_N(eV) = \sigma_N = 1/(R_d + R_b + R_b')$ .

Now we study the influence of the resonant proximity effect on tunneling conductance as well as the DOS in the DF region. The resonant proximity effect was discussed in [80] and can be characterized as follows. When the proximity



effect is weak ( $R_d/R_b \ll 1$ ), the resonant condition is given by  $R_d/R_b \sim 2h/E_{Th}$  due to the exchange splitting of DOS in different spin sub-bands. When the proximity effect is strong ( $R_d/R_b \gg 1$ ), the condition is given by  $E_{Th} \sim h$  and is realized when the length of a ferromagnet is equal to the coherence length  $\xi_F = \sqrt{D/\hbar}$ . We choose  $R_d/R_b = 1$  as a typical value to study the weak proximity regime. We also choose  $R_d/R_b = 5$  to study the strong one. We fix  $Z = Z' = 3$  because these parameters do not change the results qualitatively and consider the case of high barrier at the N/DF interface,  $R_d/R'_b = 0.1$ , in order to enhance the proximity effect.

Let us first choose the weak proximity regime and relatively small Thouless energy,  $E_{Th}/\Delta = 0.01$ . In this case the resonant condition is satisfied for  $h/E_{Th} = 0.5$ . In Fig. 4 we show the tunneling conductance for  $R_d/R_b = 1$ ,  $E_{Th}/\Delta = 0.01$  and various  $h/E_{Th}$  in (a). The ZBCD occur due to the proximity effect for  $h = 0$ . For  $h/E_{Th} = 0.5$ , the resonant ZBCP appears and split into two peaks or dips at  $eV \sim \pm h$  with increasing  $h/E_{Th}$ . The value of the resonant ZBCP exceeds unity. Note that ZBCP due to the conventional proximity effect in DN/S junctions is always less than unity [21,45] and therefore is qualitatively different from the resonant ZBCP in the DF/S junctions.

The corresponding normalized DOS of the DF is shown in (b) and (c) of Fig. 4. Note that in the DN/S junctions, the proximity effect is almost independent on  $Z$  parameter [45]. We have checked numerically that this also holds for the proximity effect in DF/S junctions. Fig. 4 displays the DOS for  $Z = 3$ ,  $R_d/R_b = 1$  and  $E_{Th}/\Delta = 0.01$  with (b)  $h/E_{Th} = 0$  and (c)  $h/E_{Th} = 0.5$  corresponding to the resonant condition. For  $h = 0$ , a sharp dip appears at zero energy over the whole DF region. For nonzero energy, the DOS is almost unity and spatially independent. For  $h/E_{Th} = 0.5$  a zero energy peak appears in the region of DF near the DF/N interface. This peak is responsible for the large ZBCP shown in (a). Therefore, the ZBCP in DF/S junctions has different physical origin compared to the one in DN/S junctions.

Next we choose the strong proximity regime and relatively small Thouless energy,  $E_{Th}/\Delta = 0.01$ . In the present case, the resonant ZBCP is expected for  $h/E_{Th} = 1$ . Fig. 5 displays the tunneling conductance for  $R_d/R_b = 5$  and  $E_{Th}/\Delta = 0.01$  and various  $h/E_{Th}$  in (a). We can find resonant ZBCP and splitting of the peak as shown in (a). The corresponding DOS is shown in (b)  $h/E_{Th} = 0$  and (c)  $h/E_{Th} = 1$ . For  $h = 0$ , a sharp dip appears at zero energy. For finite energy the DOS is almost unity and spatially independent. For  $h/E_{Th} = 1$  a peak occurs at zero energy in the range of  $x$  near the DF/N interface. We can find a similar structure in the corresponding conductance as shown in Fig. 5(a). The DOS around zero energy is strongly suppressed at the DF/S interface ( $x = L$ ) compared to the one in Fig. 4.

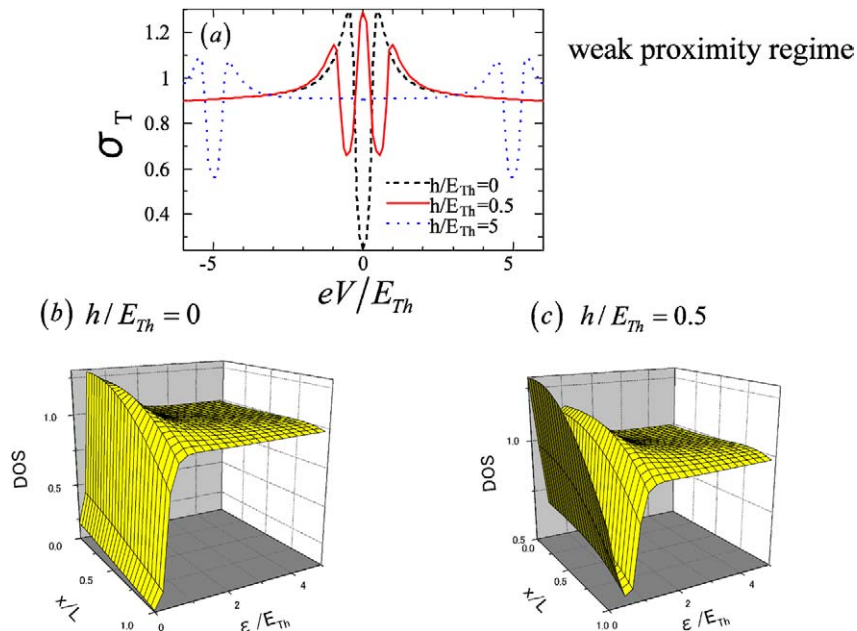


Fig. 4. Normalized tunneling conductance (a) and the DOS ((b) and (c)) with  $R_d/R_b = 1$  and  $E_{Th}/\Delta = 0.01$ . (b)  $h/E_{Th} = 0$  and (c)  $h/E_{Th} = 0.5$ .

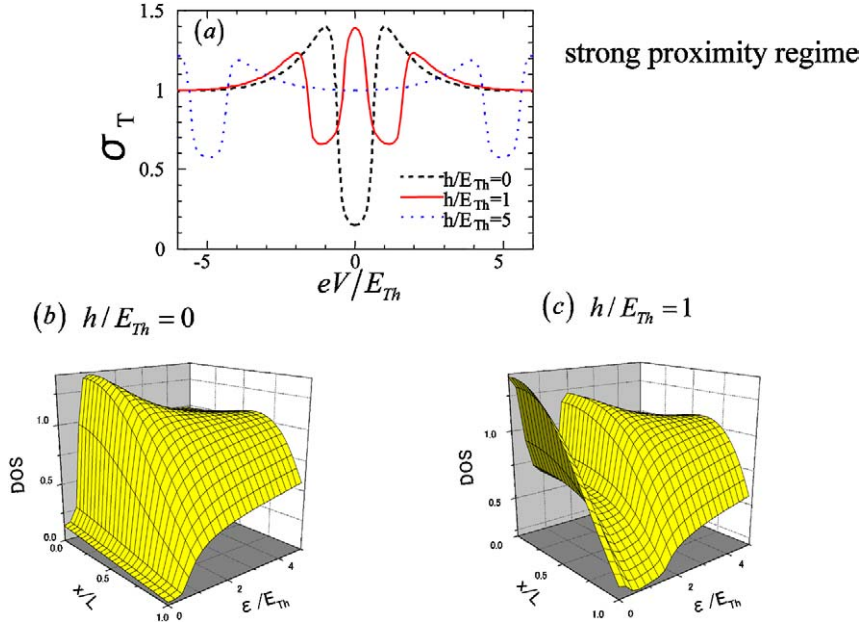


Fig. 5. Normalized tunneling conductance (a) and the DOS ((b) and (c)) with  $R_d/R_b = 5$  and  $E_{Th}/\Delta = 0.01$ . (b)  $h/E_{Th} = 0$  and (c)  $h/E_{Th} = 1$ .

Let us proceed to study the  $d$ -wave junctions both for weak and strong proximity regimes. In this case, depending on the orientation angle  $\alpha$ , the proximity effect is drastically changed: As  $\alpha$  increases the proximity effect reduces [50,51]. For  $\alpha = 0$  we can expect similar results to those in the  $s$ -wave junctions since proximity effect exists while the MARS is absent. In contrast, the tunneling conductance for large  $\alpha$  is almost independent of  $h/E_{Th}$ . Especially, the conductance is independent of  $h$  for  $\alpha/\pi = 0.25$  due to the complete absence of the proximity effect. There exist two different origins for ZBCP in DF/D junctions: the ZBCP by resonant proximity effect peculiar to DF and the ZBCP by the MARS formed at DF/D interface. When  $\alpha$  deviates from 0, the MARS are formed at the interface. At the same time, the proximity effect is suppressed due to the competition between the proximity effect and the MARS. Therefore the MARS provide the dominant contribution to the ZBCP compared to the resonant proximity effect in DF, as will be discussed below.

First we choose the weak proximity regime where the resonant condition is  $h/E_{Th} = 0.5$ . Fig. 6 displays the tunneling conductance for  $R_d/R_b = 1$ ,  $E_{Th}/\Delta = 0.01$  and various  $\alpha$  with (a)  $h/E_{Th} = 0$  and (b)  $h/E_{Th} = 0.5$ . For  $h = 0$ , ZBCP appears for  $\alpha/\pi = 0$  due to the proximity effect as in the case of the  $s$ -wave junctions while ZBCP appears for  $\alpha/\pi = 0.25$  due to the formation of the MARS (Fig. 6(a)). For  $h/E_{Th} = 0.5$ , the height of the ZBCP by the resonant proximity effect for  $\alpha = 0$  exceeds the one by MARS for  $\alpha/\pi = 0.25$  (Fig. 6(b)) in contrast to the ballistic junctions where the ZBCP for  $\alpha/\pi = 0.25$  is most enhanced [3].

We also study the DOS of the DF for the same parameters as those of Fig. 6(b) as shown in (c)  $\alpha/\pi = 0$  and (d)  $\alpha/\pi = 0.125$  in Fig. 6. The line shapes of the LDOS near the DF/S interface are qualitatively similar to the tunneling conductance. For  $\alpha/\pi = 0$  a zero-energy peak appears as in the case of  $s$ -wave junctions. With increasing  $\alpha$ , the DOS around the zero energy is suppressed due to the reduction of the proximity effect. The extreme case is  $\alpha/\pi = 0.25$ , where the DOS is always unity since the proximity effect is completely absent.

Next we look at the junctions for the strong proximity regime. In Fig. 7 we show the tunneling conductance for  $R_d/R_b = 5$ ,  $E_{Th}/\Delta = 0.01$  and various  $\alpha$  with (a)  $h/E_{Th} = 0$  and (b)  $h/E_{Th} = 1$ . In this case we also find the ZBCP for  $\alpha = 0$  by the resonant proximity effect. The height of the ZBCP is suppressed as  $\alpha$  increases as shown in Figs. 7(b).

The corresponding DOS of the DF to the case of (b) in Fig. 7 is shown in Fig. 7 with (c)  $\alpha/\pi = 0$  and (d)  $\alpha/\pi = 0.125$ . For  $\alpha = 0$  the structure of the DOS at  $x = 0$  reflects the line shapes of the tunneling conductance. With increasing  $\alpha$  the zero energy peak of the DOS becomes suppressed. The DOS at the DF/S interface ( $x = L$ ) are drastically suppressed compared to those in Fig. 6.

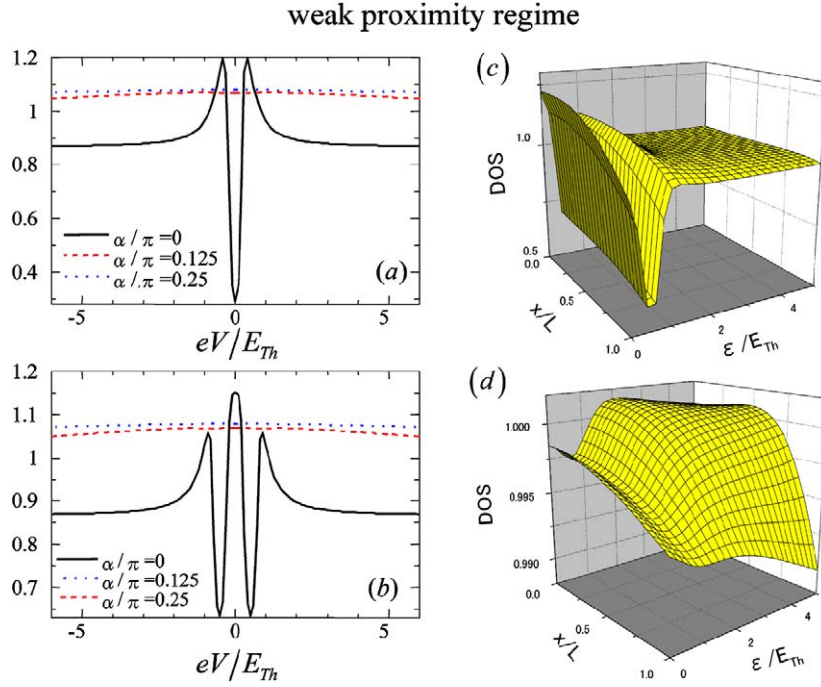


Fig. 6. Normalized tunneling conductance ((a) and (b)) and the DOS ((c) and (d)) for  $d$ -wave superconductors with  $R_d/R_b = 1$  and  $E_{Th}/\Delta = 0.01$ . (a)  $h/E_{Th} = 0$ , (b)  $h/E_{Th} = 1$ , (c)  $h/E_{Th} = 1$  and  $\alpha/\pi = 0$  and (d)  $h/E_{Th} = 1$  and  $\alpha/\pi = 0.125$ .

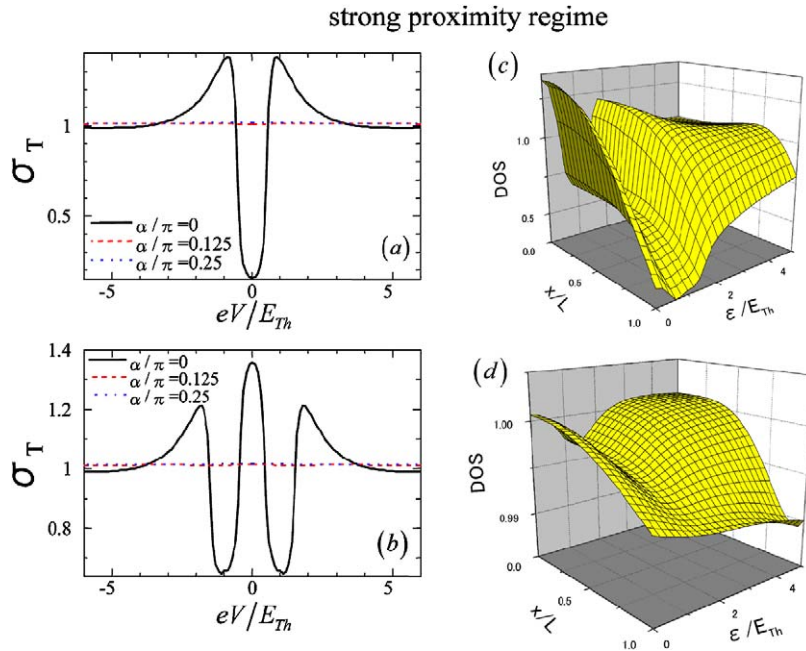


Fig. 7. Normalized tunneling conductance ((a) and (b)) and the DOS ((c) and (d)) for  $d$ -wave superconductors with  $R_d/R_b = 5$  and  $E_{Th}/\Delta = 0.01$ . (a)  $h/E_{Th} = 0$ , (b)  $h/E_{Th} = 1$ , (c)  $h/E_{Th} = 1$  and  $\alpha/\pi = 0$  and (d)  $h/E_{Th} = 1$  and  $\alpha/\pi = 0.125$ .

#### 4. Conclusions

In this article we studied the tunneling conductance in F/S, F/D and 2DEG/S junctions in ballistic regime. We extended the BTK formula and calculated the tunneling conductance of the junctions. We clarified the following points:

- The exchange field always suppresses the conductance in F/S and F/D junctions.
- In 2DEG/S junctions, for low insulating barrier the RSOC suppresses the tunneling conductance while for high insulating barrier it can slightly enhance the tunneling conductance. We also found a re-entrant behavior of the conductance at zero voltage as a function of RSOC for intermediate insulating barrier strength. The results give the possibility of controlling the AR probability by a gate voltage. We believe that the obtained results are useful for a better understanding of related experiments of mesoscopic F/S and 2DEG/S junctions.

In the latter part of the present article, a detailed theoretical study of the tunneling conductance and the density of states in normal metal/diffusive ferromagnet/*s*- and *d*-wave superconductor junctions is presented. We clarified that the resonant proximity effect strongly influences the tunneling conductance and the density of states. There are several points which have been clarified in this article:

- For *s*-wave junctions, due to the resonant proximity effect, a sharp ZBCP appears for small  $E_{\text{Th}}$ . We showed that the mechanism of the ZBCP in DF/S junctions is essentially different from that in DN/S junctions and is due to the strong enhancement of the DOS at a certain value of the exchange field. As a result, the magnitude of the ZBCP in DF/S junctions can exceed unity in contrast to that in DN/S junctions.
- For *d*-wave junctions at  $\alpha = 0$ , similar to the *s*-wave case, the sharp ZBCP is formed when the resonant condition is satisfied. At finite misorientation angle  $\alpha$ , the MARS contribute to the conductance when  $R_d/R_b \ll 1$  and  $Z \gg 1$ . With the increase of  $\alpha$  the contribution of the resonant proximity effect becomes smaller while the MARS dominate the conductance. As a result, for sufficiently large  $\alpha$  ZBCP exists independently of whether the resonant condition is satisfied or not. In the opposite case of the weak barrier,  $R_d/R_b \gg 1$ , the contribution of MARS is negligible and ZBCP appears only when the resonant condition is satisfied.

An interesting problem is a calculation of the tunneling conductance in normal metal/diffusive ferromagnet/*p*-wave superconductor junctions because interesting phenomena were predicted in diffusive normal metal/*p*-wave superconductor junctions [52]. We will perform it in the near future.

## Acknowledgements

The authors appreciate useful and fruitful discussions with J. Inoue, Yu. Nazarov and A. Golubov. This work was supported by NAREGI Nanoscience Project, the Ministry of Education, Culture, Sports, Science and Technology, Japan, the Core Research for Evolutional Science and Technology (CREST) of the Japan Science and Technology Corporation (JST) and a Grant-in-Aid for the 21st Century COE “Frontiers of Computational Science”. The computational aspect of this work has been performed at the Research Center for Computational Science, Okazaki National Research Institutes and the facilities of the Supercomputer Center, Institute for Solid State Physics, University of Tokyo and the Computer Center.

## References

- [1] A.F. Andreev, Sov. Phys. JETP 19 (1964) 1228.
- [2] G.E. Blonder, M. Tinkham, T.M. Klapwijk, Phys. Rev. B 25 (1982) 4515.
- [3] Y. Tanaka, S. Kashiwaya, Phys. Rev. Lett. 74 (1995) 3451;  
S. Kashiwaya, Y. Tanaka, M. Koyanagi, K. Kajimura, Phys. Rev. B 53 (1996) 2667;  
Y. Tanuma, Y. Tanaka, S. Kashiwaya, Phys. Rev. B 64 (2001) 214519.
- [4] T. Hirai, Y. Tanaka, N. Yoshida, Y. Asano, J. Inoue, S. Kashiwaya, Phys. Rev. B 67 (2003) 174501;  
N. Yoshida, Y. Tanaka, J. Inoue, S. Kashiwaya, J. Phys. Soc. Jpn. 68 (1999) 1071;  
S. Kashiwaya, Y. Tanaka, N. Yoshida, M.R. Beasley, Phys. Rev. B 60 (1999) 3572;  
I. Zutic, O.T. Valls, Phys. Rev. B 60 (1999) 6320;  
I. Zutic, O.T. Valls, Phys. Rev. B 61 (2000) 1555;  
N. Stefanakis, Phys. Rev. B 64 (2001) 224502;  
N. Stefanakis, J. Phys. Condens. Matter 13 (2001) 3643.
- [5] P.M. Tedrow, R. Meservey, Phys. Rev. Lett. 26 (1971) 192;  
P.M. Tedrow, R. Meservey, Phys. Rev. B 7 (1973) 318;  
R. Meservey, P.M. Tedrow, Phys. Rep. 238 (1994) 173.
- [6] S.K. Upadhyay, A. Palanisami, R.N. Louie, R.A. Buhrman, Phys. Rev. Lett. 81 (1998) 3247.

- [7] R.J. Soulen Jr., J.M. Byers, M.S. Osofsky, B. Nadgorny, T. Ambrose, S.F. Cheng, P.R. Broussard, C.T. Tanaka, J. Nowak, J.S. Moodera, A. Barry, J.M.D. Coey, *Science* 282 (1998) 85.
- [8] M.J.M. de Jong, C.W.J. Beenakker, *Phys. Rev. Lett.* 74 (1995) 1657.
- [9] J.E. Hirsch, *Phys. Rev. Lett.* 83 (1999) 1834.
- [10] P. Streda, P. Seba, *Phys. Rev. Lett.* 90 (2003) 256601.
- [11] J. Schliemann, D. Loss, *Phys. Rev. B* 68 (2003) 165311.
- [12] J. Sinova, D. Culcer, Q. Niu, N.A. Sinitsyn, T. Jungwirth, A.H. MacDonald, *Phys. Rev. Lett.* 92 (2004) 126603.
- [13] E.I. Rashba, *Fiz. Tverd. Tela (Leningrad)* 2 (1960) 1224;  
E.I. Rashba, *Sov. Phys. Solid State* 2 (1960) 1109;  
Yu.A. Bychkov, E.I. Rashba, *J. Phys. C* 17 (1984) 6039.
- [14] S. Datta, B. Das, *Appl. Phys. Lett.* 56 (1990) 665.
- [15] L.W. Molenkamp, G. Schmidt, G.E.W. Bauer, *Phys. Rev. B* 64 (2001) 121202.
- [16] V.M. Edelstein, *Solid State Commun.* 73 (1990) 233.
- [17] J. Inoue, G.E.W. Bauer, L.W. Molenkamp, *Phys. Rev. B* 67 (2003) 033104;  
J. Inoue, G.E.W. Bauer, L.W. Molenkamp, *Phys. Rev. B* 70 (2004) 041303.
- [18] F.W.J. Hekking, Yu.V. Nazarov, *Phys. Rev. Lett.* 71 (1993) 1625.
- [19] F. Giazotto, P. Pingue, F. Beltram, M. Lazzarino, D. Orani, S. Rubini, A. Franciosi, *Phys. Rev. Lett.* 87 (2001) 216808.
- [20] T.M. Klapwijk, *Physica B* 197 (1994) 481.
- [21] A. Kastalsky, A.W. Kleinsasser, L.H. Greene, R. Bhat, F.P. Milliken, J.P. Harbison, *Phys. Rev. Lett.* 67 (1991) 3026.
- [22] C. Nguyen, H. Kroemer, E.L. Hu, *Phys. Rev. Lett.* 69 (1992) 2847.
- [23] B.J. van Wees, P. de Vries, P. Magnee, T.M. Klapwijk, *Phys. Rev. Lett.* 69 (1992) 510.
- [24] J. Nitta, T. Akazaki, H. Takayanagi, *Phys. Rev. B* 49 (1994) 3659.
- [25] S.J.M. Bakker, E. van der Drift, T.M. Klapwijk, H.M. Jaeger, S. Radelaar, *Phys. Rev. B* 49 (1994) 13275.
- [26] P. Xiong, G. Xiao, R.B. Laibowitz, *Phys. Rev. Lett.* 71 (1993) 1907.
- [27] P.H.C. Magnee, N. van der Post, P.H.M. Kooistra, B.J. van Wees, T.M. Klapwijk, *Phys. Rev. B* 50 (1994) 4594.
- [28] J. Kutchinsky, R. Taboryski, T. Clausen, C.B. Sorensen, A. Kristensen, P.E. Lindelof, J. Bindslev Hansen, C. Schelde Jacobsen, J.L. Skov, *Phys. Rev. Lett.* 78 (1997) 931.
- [29] W. Poirier, D. Mailly, M. Sanquer, *Phys. Rev. Lett.* 79 (1997) 2105.
- [30] G. Eilenberger, *Z. Phys.* 214 (1968) 195.
- [31] G.M. Eliashberg, *Sov. Phys. JETP* 34 (1971) 668.
- [32] A.I. Larkin, Yu.V. Ovchinnikov, *Sov. Phys. JETP* 41 (1975) 960.
- [33] K.D. Usadel, *Phys. Rev. Lett.* 25 (1970) 507.
- [34] A.F. Volkov, A.V. Zaitsev, T.M. Klapwijk, *Physica C* 210 (1993) 21.
- [35] M.Yu. Kupriyanov, V.F. Lukichev, *Zh. Exp. Teor. Fiz.* 94 (1988) 139;  
M.Yu. Kupriyanov, V.F. Lukichev, *Sov. Phys. JETP* 67 (1988) 1163.
- [36] Yu.V. Nazarov, *Phys. Rev. Lett.* 73 (1994) 1420.
- [37] S. Yip, *Phys. Rev. B* 52 (1995) 3087.
- [38] Yu.V. Nazarov, T.H. Stoof, *Phys. Rev. Lett.* 76 (1996) 823;  
T.H. Stoof, Yu.V. Nazarov, *Phys. Rev. B* 53 (1996) 14496.
- [39] A.F. Volkov, N. Allsopp, C.J. Lambert, *J. Phys. Condens. Matter* 8 (1996) L45;  
A.F. Volkov, H. Takayanagi, *Phys. Rev. B* 56 (1997) 11184.
- [40] A.A. Golubov, F.K. Wilhelm, A.D. Zaikin, *Phys. Rev. B* 55 (1997) 1123.
- [41] A.F. Volkov, H. Takayanagi, *Phys. Rev. B* 56 (1997) 11184.
- [42] E.V. Bezuglyi, E.N. Bratus', V.S. Shumeiko, G. Wendin, H. Takayanagi, *Phys. Rev. B* 62 (2000) 14439.
- [43] R. Seviour, A.F. Volkov, *Phys. Rev. B* 61 (2000) R9273.
- [44] W. Belzig, F.K. Wilhelm, C. Bruder, et al., *Superlattices and Microstructures* 25 (1999) 1251.
- [45] Y. Tanaka, A.A. Golubov, S. Kashiwaya, *Phys. Rev. B* 68 (2003) 054513.
- [46] Yu.V. Nazarov, *Superlattices and Microstructures* 25 (1999) 1221, cond-mat/9811155.
- [47] L.J. Buchholtz, G. Zwicknagl, *Phys. Rev. B* 23 (1981) 5788;  
C. Bruder, *Phys. Rev. B* 41 (1990) 4017;  
C.R. Hu, *Phys. Rev. Lett.* 72 (1994) 1526.
- [48] S. Kashiwaya, Y. Tanaka, *Rep. Prog. Phys.* 63 (2000) 1641 and references therein.
- [49] J. Geerk, X.X. Xi, G. Linker, *Z. Phys. B* 73 (1988) 329;  
S. Kashiwaya, Y. Tanaka, M. Koyanagi, H. Takashima, K. Kajimura, *Phys. Rev. B* 51 (1995) 1350;  
L. Alff, H. Takashima, S. Kashiwaya, N. Terada, H. Ihara, Y. Tanaka, M. Koyanagi, K. Kajimura, *Phys. Rev. B* 55 (1997) 14757;  
M. Covington, M. Aprili, E. Paraoanu, L.H. Greene, F. Xu, J. Zhu, C.A. Mirkin, *Phys. Rev. Lett.* 79 (1997) 277;  
J.Y.T. Wei, N.-C. Yeh, D.F. Garrigus, M. Strasiak, *Phys. Rev. Lett.* 81 (1998) 2542;  
I. Iguchi, W. Wang, M. Yamazaki, Y. Tanaka, S. Kashiwaya, *Phys. Rev. B* 62 (2000) R6131;  
F. Laube, G. Goll, H. v. Löhneysen, M. Fogelström, F. Lichtenberg, *Phys. Rev. Lett.* 84 (2000) 1595;  
Z.Q. Mao, K.D. Nelson, R. Jin, Y. Liu, Y. Maeno, *Phys. Rev. Lett.* 87 (2001) 037003;  
Ch. Wälti, H.R. Ott, Z. Fisk, J.L. Smith, *Phys. Rev. Lett.* 84 (2000) 5616;  
H. Aubin, L.H. Greene, Sha Jian, D.G. Hinks, *Phys. Rev. Lett.* 89 (2002) 177001;

- Z.Q. Mao, M.M. Rosario, K.D. Nelson, K. Wu, I.G. Deac, P. Schiffer, Y. Liu, T. He, K.A. Regan, R.J. Cava, *Phys. Rev. B* 67 (2003) 094502;  
 A. Sharoni, O. Millo, A. Kohen, Y. Dagan, R. Beck, G. Deutscher, G. Koren, *Phys. Rev. B* 65 (2002) 134526;  
 A. Kohen, G. Leibovitch, G. Deutscher, *Phys. Rev. Lett.* 90 (2003) 207005.
- [50] Y. Tanaka, Y.V. Nazarov, S. Kashiwaya, *Phys. Rev. Lett.* 90 (2003) 167003.
- [51] Y. Tanaka, Y. Nazarov, A. Golubov, S. Kashiwaya, *Phys. Rev. B* 69 (2004) 144519.
- [52] Y. Tanaka, S. Kashiwaya, *Phys. Rev. B* 70 (2004) 012507;  
 Y. Tanaka, S. Kashiwaya, T. Yokoyama, *Phys. Rev. B* 71 (2005) 094513.
- [53] S. Yip, *Phys. Rev. B* 52 (1995) 15504.
- [54] T. Yokoyama, Y. Tanaka, A.A. Golubov, J. Inoue, Y. Asano, *Phys. Rev. B* 71 (2005) 094506.
- [55] A.I. Buzdin, L.N. Bulaevskii, S.V. Panyukov, *Pis'ma Zh. Eksp. Teor. Phys.* 35 (1982) 147;  
 A.I. Buzdin, L.N. Bulaevskii, S.V. Panyukov, *JETP Lett.* 35 (1982) 178.
- [56] A.I. Buzdin, M.Yu. Kupriyanov, *Pis'ma Zh. Eksp. Teor. Phys.* 53 (1991) 308;  
 A.I. Buzdin, M.Yu. Kupriyanov, *JETP Lett.* 53 (1991) 321.
- [57] E.A. Demler, G.B. Arnold, M.R. Beasley, *Phys. Rev. B* 55 (15) (1997) 174.
- [58] V.V. Ryazanov, V.A. Oboznov, A.Yu. Rusanov, A.V. Veretennikov, A.A. Golubov, J. Aarts, *Phys. Rev. Lett.* 86 (2001) 2427;  
 V.V. Ryazanov, V.A. Oboznov, A.V. Veretennikov, A.Yu. Rusanov, *Phys. Rev. B* 65 (2001) 020501(R);  
 S.M. Frolov, D.J. Van Harlingen, V.A. Oboznov, V.V. Bolginov, V.V. Ryazanov, *Phys. Rev. B* 70 144505.
- [59] T. Kontos, M. Aprili, J. Lesueur, F. Genet, B. Stephanidis, R. Boursier, *Phys. Rev. Lett.* 89 (2002) 137007.
- [60] Y. Blum, A. Tsukernik, M. Karpovski, A. Palevski, *Phys. Rev. Lett.* 89 (2002) 187004.
- [61] H. Sellier, C. Baraduc, F. Lefloch, R. Calemczuk, *Phys. Rev. B* 68 (2003) 054531.
- [62] A. Bauer, J. Bentner, M. Aprili, M.L. Della Rocca, M. Reinwald, W. Wegscheider, C. Strunk, *Phys. Rev. Lett.* 92 (2004) 217001.
- [63] Z. Radovic, M. Ledvij, Lj. Dobrosavljevi-Gruji, A.I. Buzdin, J.R. Clem, *Phys. Rev. B* 44 (1991) 759.
- [64] L.R. Tagirov, *Phys. Rev. Lett.* 83 (1999) 2058.
- [65] Ya.V. Fominov, N.M. Chtchelkatchev, A.A. Golubov, *Pis'ma Zh. Eksp. Teor. Fiz.* 74 (2001) 101;  
 Ya.V. Fominov, N.M. Chtchelkatchev, A.A. Golubov, *JETP Lett.* 74 (2001) 96;  
 Ya.V. Fominov, N.M. Chtchelkatchev, A.A. Golubov, *Phys. Rev. B* 66 (2002) 014507.
- [66] A. Rusanov, R. Boogaard, M. Hesselberth, H. Sellier, J. Aarts, *Physica C* 36 (9) (2002) 300.
- [67] V.V. Ryazanov, V.A. Oboznov, A.S. Prokofiev, S.V. Dubonos, *JETP Lett.* 77 (2003) 39.
- [68] A. Kadigrobov, R.I. Shekhter, M. Jonson, Z.G. Ivanov, *Phys. Rev. B* 60 (1999) 14593.
- [69] R. Seviour, C.J. Lambert, A.F. Volkov, *Phys. Rev. B* 59 (1999) 6031.
- [70] M. Leadbeater, C.J. Lambert, K.E. Nagaev, R. Raimondi, A.F. Volkov, *Phys. Rev. B* 59 (1999) 12264.
- [71] F.S. Bergeret, K.B. Efetov, A.I. Larkin, *Phys. Rev. B* 62 (2000) 11872;  
 F.S. Bergeret, A.F. Volkov, K.B. Efetov, *Phys. Rev. Lett.* 86 (2001) 4096.
- [72] A. Kadigrobov, R.I. Shekhter, M. Jonson, *Europhys. Lett.* 54 (2001) 394.
- [73] A. Buzdin, *Phys. Rev. B* 62 (11) (2000) 377.
- [74] M. Zareyan, W. Belzig, Yu.V. Nazarov, *Phys. Rev. Lett.* 86 (2001) 308;  
 M. Zareyan, W. Belzig, Yu.V. Nazarov, *Phys. Rev. B* 65 (2002) 184505.
- [75] A.I. Baladie, A. Buzdin, *Phys. Rev. B* 64 (2001) 224514.
- [76] F.S. Bergeret, A.F. Volkov, K.B. Efetov, *Phys. Rev. B* 65 (2002) 134505.
- [77] A.A. Golubov, M.Yu. Kupriyanov, Ya.V. Fominov, *JETP Lett.* 75 (2002) 223.
- [78] V.N. Krivoruchko, E.A. Koshina, *Phys. Rev. B* 66 (2002) 014521.
- [79] T. Kontos, M. Aprili, J. Lesueur, X. Grison, *Phys. Rev. Lett.* 86 (2001) 304;  
 T. Kontos, M. Aprili, J. Lesueur, X. Grison, L. Dumoulin, *Phys. Rev. Lett.* 93 (2004) 137001.
- [80] T. Yokoyama, Y. Tanaka, A.A. Golubov, *Phys. Rev. B* 72 (2005) 052512.